Electronic Supplementary Material (ESI) for Journal of Materials Chemistry A.

Supplementary information: Direct Monitoring of the Potassium Charge Carrier in Prussian Blue Cathodes using Potassium K-edge X-ray Absorption Spectroscopy

Alexander J. Mayer [a,b], Owain T. Beynon [c], Andrew J. Logsdail [c], Upul Wijayantha [a,d], Sandra E. Dann [a], José F. Marco [e], Joshua Elliott [b], Matteo Aramini [b], Giannantonio Cibin [b], & Simon A. Kondrat [a,*]

a) Department of Chemistry, Loughborough University, Loughborough, Leicestershire, LE113TU, UK; b) Diamond Light Source, Harwell Science and Innovation Campus, Chilton, Didcot, OX11 0DE, UK; c) Cardiff Catalysis Institute, School of Chemistry, Cardiff University, Park Place, Cardiff, CF103AT, Wales, UK ; d) Centre for Renewable and Low Carbon Energy, Cranfield University, Cranfield, Bedfordshire, MK43 0AL, U.K; e) Instituto de Quimica Fisica Rocasolano, CSIC, Serrano, 119, 28006 Madrid, Spain

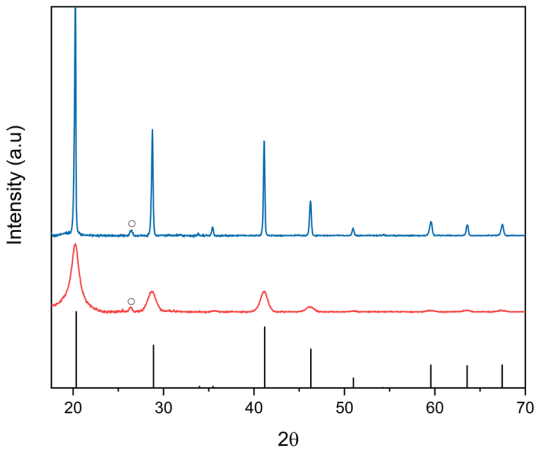

Figure S 1. XRD patterns of LC-PB (Blue) and SC-PB (Red). Reference pattern of Prussian Blue, JCPDS no. 52-1907 (Black), circle represents a peak from tape from the instrument.

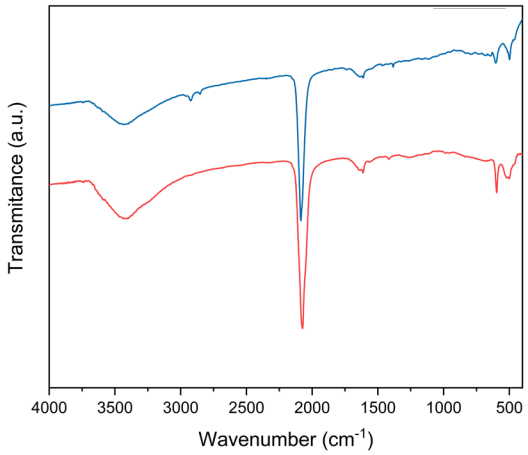

Figure S 2. ATR-IR spectra of LC-PB (Blue) and SC-PB (Red)

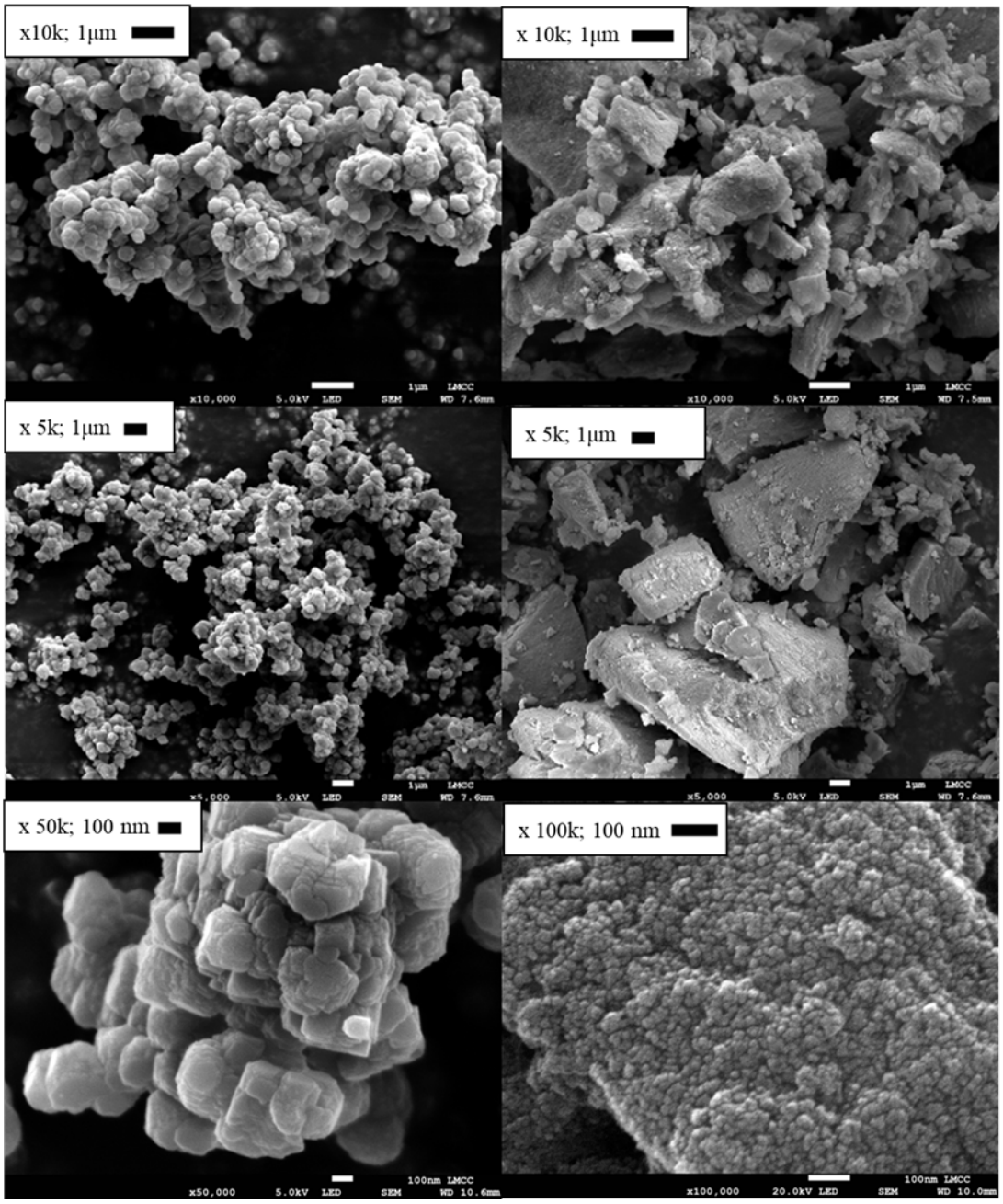

Figure S 3. SEM images of LC-PB (left-hand side) and SC-PB (right-hand side) powders.

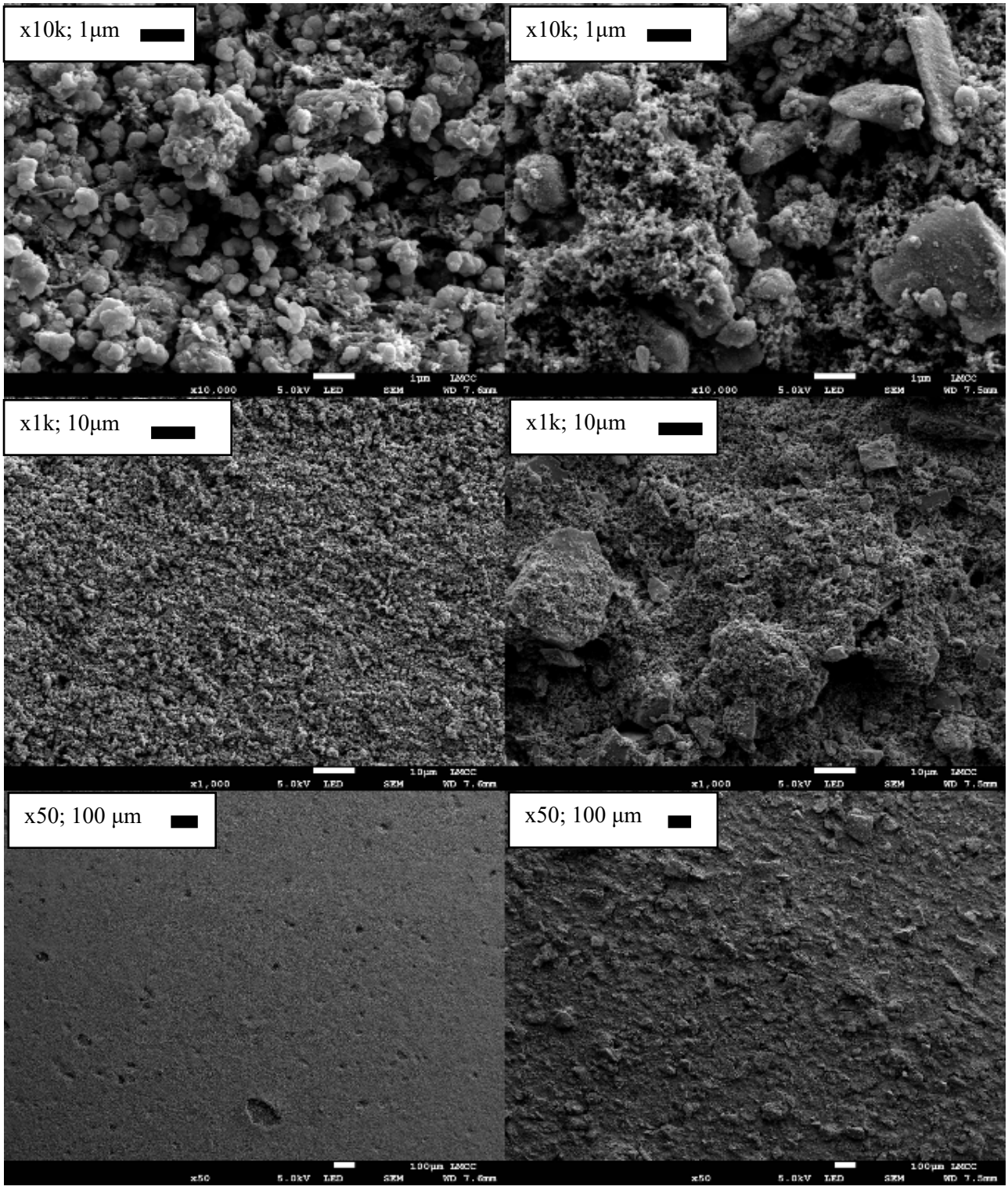

Figure S 4. SEM images of fresh electrodes of LC-PB (left hand-side) and SC-PB (right-hand side).

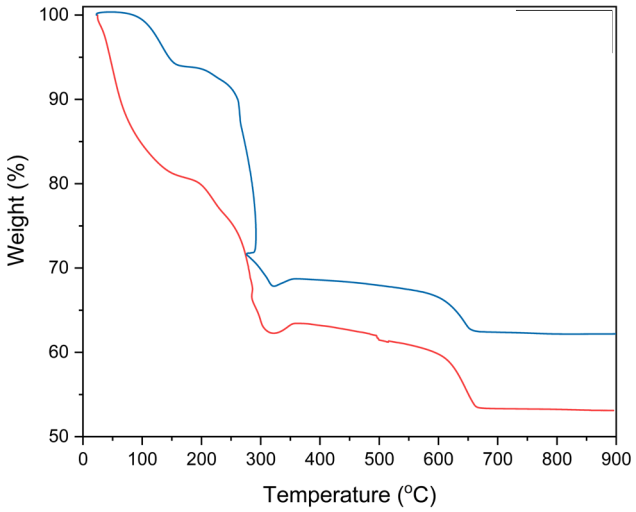

Figure S 5. Thermogravimetric analysis (TGA) of LC-PB (Blue) and SC-PB (red) run in air.

Table S 1. Crystallite and particle sizes determined by Scherrer equation from XRD and particle size from SEM analysis.

Samples	Particle size (nm)	Crystallite size (nm)	BET Surface area (m^2/g)
LC-PB	140(30)	103(3)	73
SC-PB	19(4)	12(1)	165

Table S 21. MP-AES and CHN analysis of C-PB and D-PB.

Samples	Potassium (wt %)	Iron (wt %)	Carbon (wt %)	Nitrogen (wt %)	Hydrogen (wt %)	Water (wt %)
LC-PB	6.4(2)	31.8(7)	19.7(2)	22.8(1)	1.2(1)	17.71
SC-PB	11.1(8)	29.8(8)	18.3(2)	21.7(1)	0.6(1)	20.14

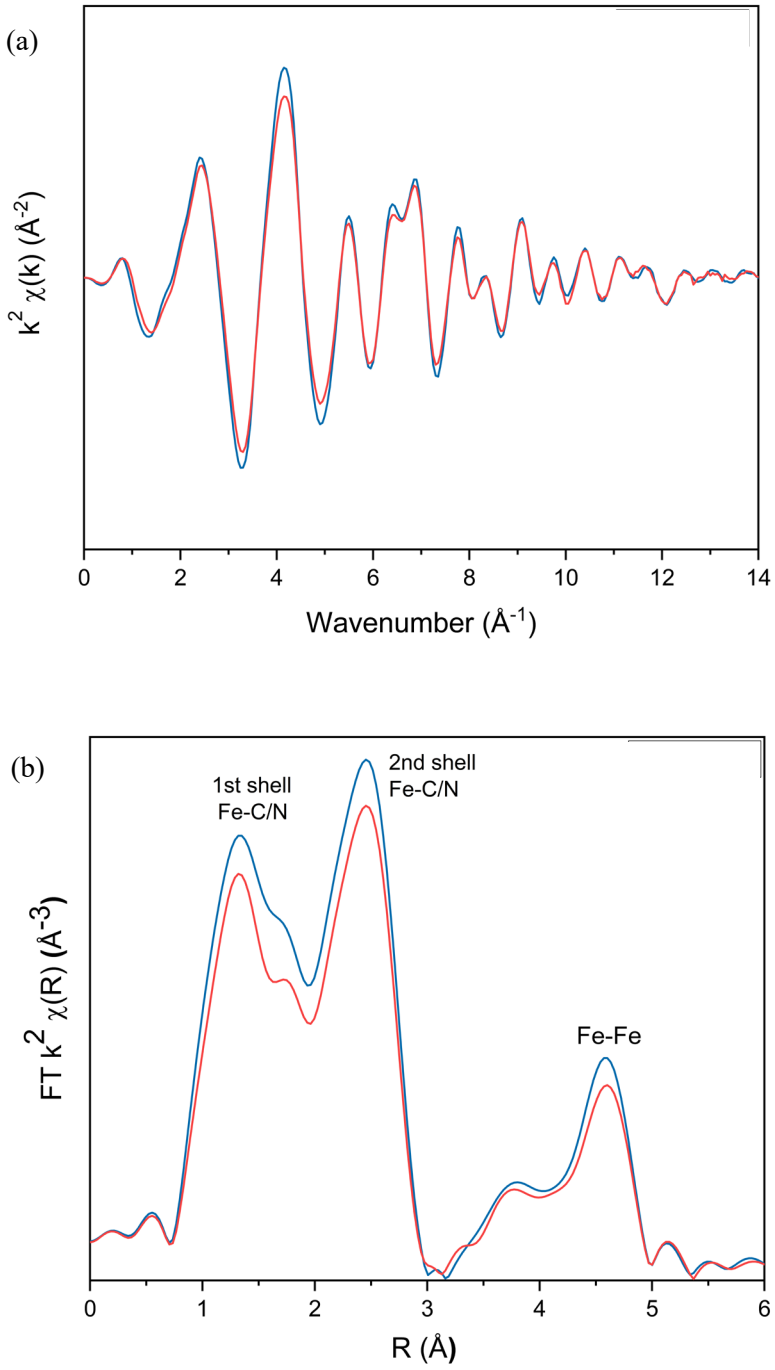

Figure S 6 Fe K edge EXAFS of (a) k space, (b) Fourier Transform χR of LC-PB powder (Blue), SC-PB powder (Red).

Table S3.- Hyperfine parameters obtained from the fit of the spectra presented in Figure 1b. (δ is the isomer shift; Δ is the quadrupole splitting and Γ is the full with at half maximum).

SAMPLE	Site	δ (mm s^{-1})	Δ (mm s^{-1})	Γ (mms s^{-1})	Area (%)
LC-PB	LS Fe(II)	-0.15	--	0.29	51
	HS Fe(III) S1	0.40	0.12	0.29	28
	HS Fe(III) S2	0.40	0.52	0.29	21
SC-PB	LS Fe(II)	-0.14	--	0.28	50
	HS Fe(III) S1	0.41	0.15	0.28	29
	HS Fe(III) S2	0.41	0.56	0.28	21
LC-PB used	LS Fe(II)	-0.14	--	0.29	49
	HS Fe(III) S1	0.41	0.13	0.29	34
	HS Fe(III) S2	0.41	0.51	0.29	17
SC-PB used	LS Fe(II)	-0.15	--	0.29	25
	HS Fe(III) S1	0.43	0.19	0.29	20
	HS Fe(III) S2	0.38	0.55	0.29	35
	HS Fe(III) S3	0.39	0.86	0.29	20

Table S4.- Average isomer shift and quadrupole splitting of the HS Fe(III) components in the spectra shown in Figure 1b. A_{III}/A_{II} is the $Area_{Fe(III)}/Area_{Fe(II)}$ ratio.

SAMPLE	**Site**	**δ (mm s^{-1})**	**<Δ> (mm s^{-1})**	**A_{III}/A_{II}**
LC-PB	HS Fe(III)	0.40	0.29	0.96
SC-PB	HS Fe(III)	0.41	0.32	1.00
LC-PB used	HS Fe(III)	0.41	0.26	1.04
SC-PB used	HS Fe(III)	0.40	0.54	3

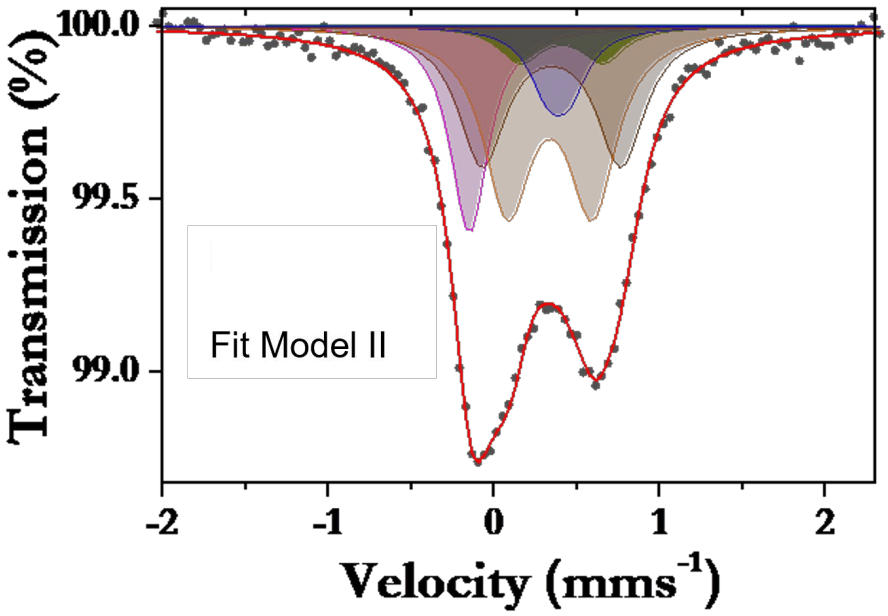

Figure S7.- Room temperature Mössbauer spectra recorded from sample SC-PB used fitted to a different model than that shown in Figure 1b (main paper). The dark and light brown doublets correspond to Ferrihydrite. The remaining components correspond to SC-PB fresh. The Mössbauer parameters and relative area ratios of the SC-PB fresh have been fixed to those deduced from the spectrum of SC-PB fresh.

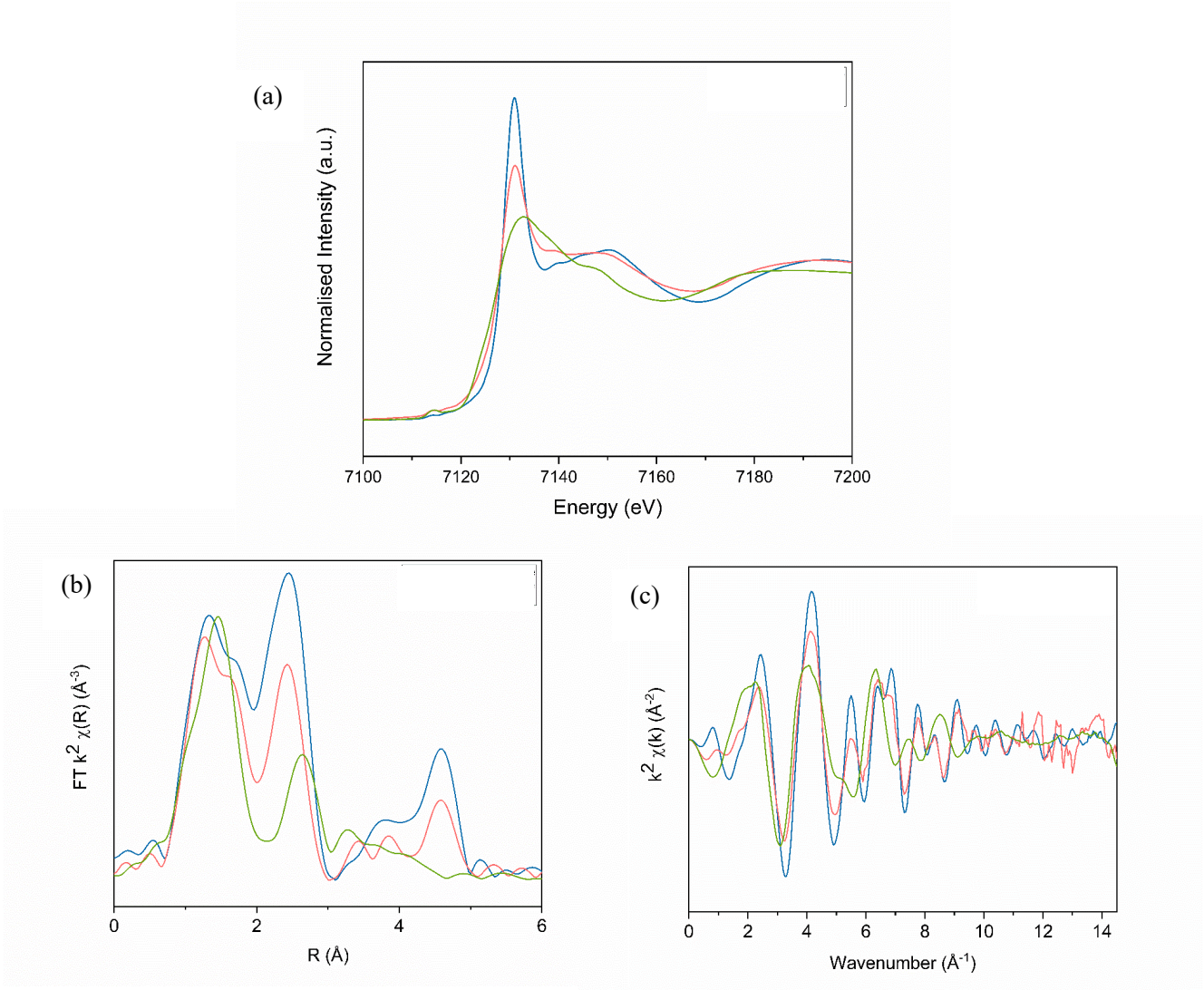

Figure S8 Fe K edge XAFS of LC-PB before and after cycling in comparison to a Ferrihydrite standard (a) XANES, (b) k space, (c) Fourier Transform χR. LC-PB powder (Blue), SC-PB powder (Red), Ferrihydrite (Green)

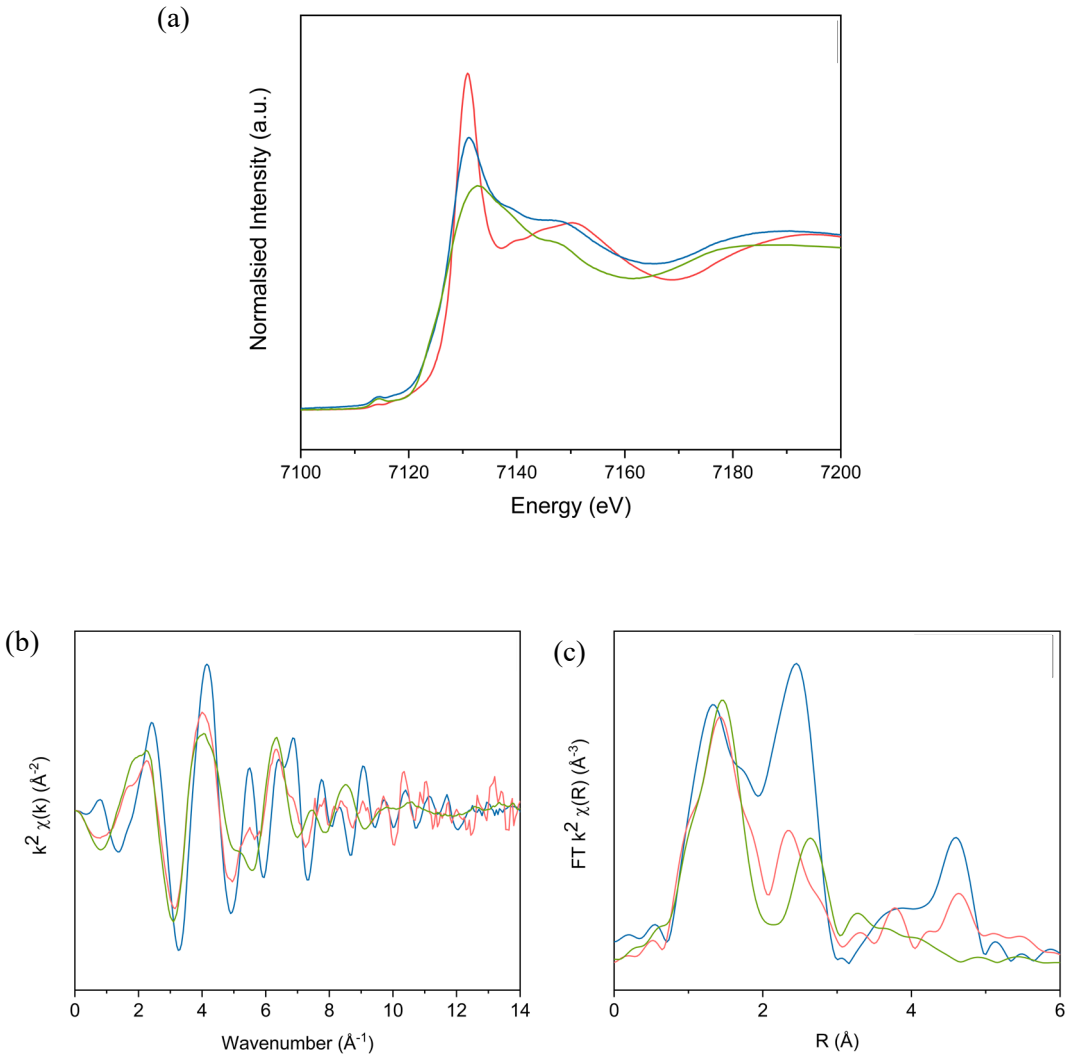

Figure S 9 Fe K edge XAFS of SC-PB before and after cycling in comparison to a Ferrihydrite standard

(a) XANES, (b) k space, (c) Fourier Transform χR. SC-PB powder (Blue), SC-PB powder (Red), Ferrihydrite (Green)

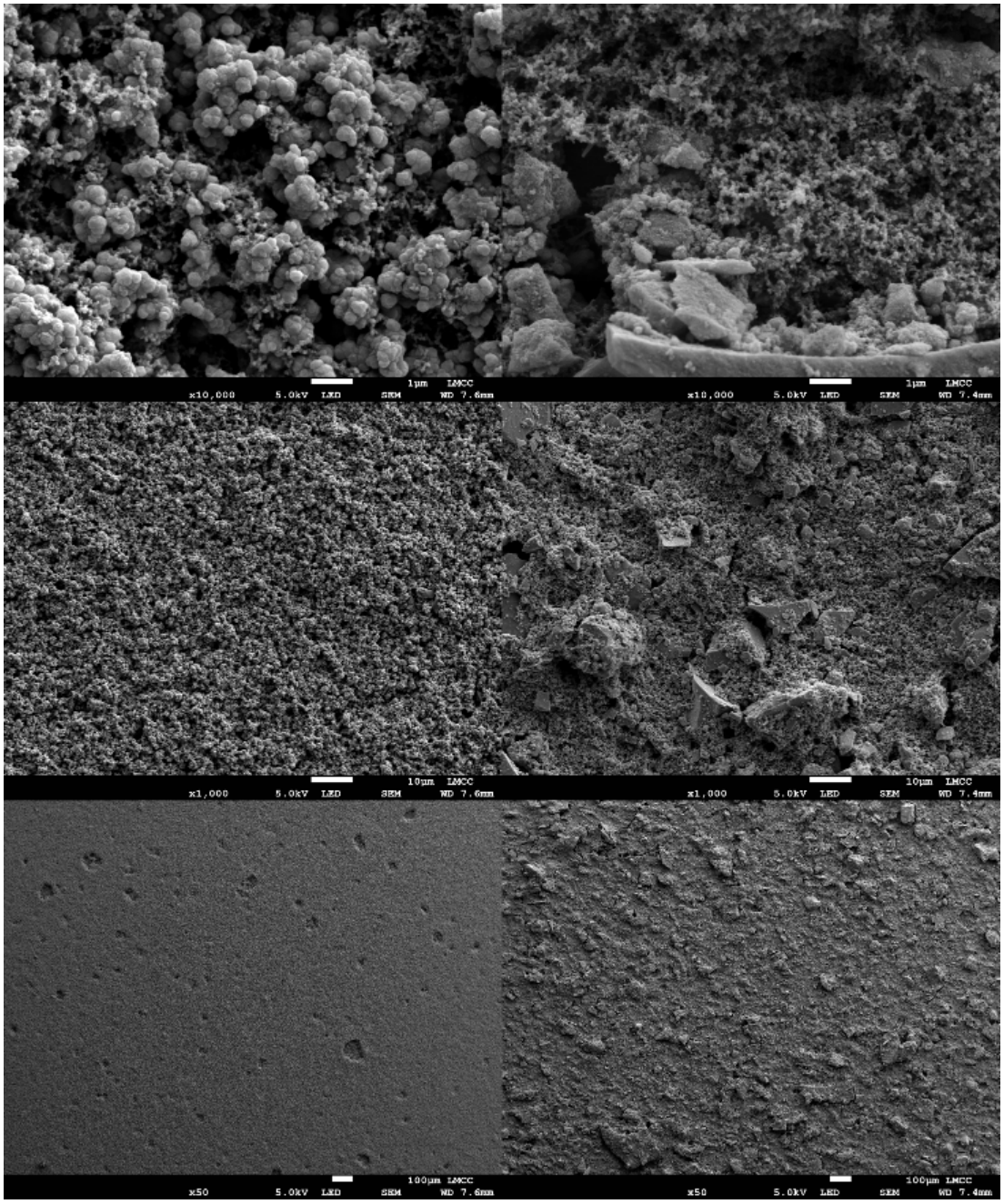

Figure S 10. SEM images of used electrodes of LC-PB (left-hand side) and SC-PB (right-hand side).

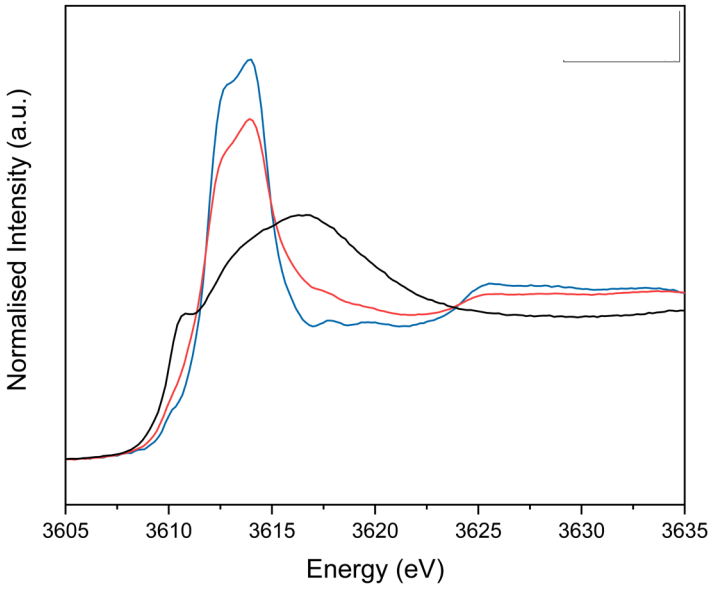

Figure S 11. Comparing potassium k edge XANES collected using a total electron yield detector of LC-PB (Blue), SC-PB (red), and 0.1 M KNO_3 (aq) electrolyte (Black).

Figure *S12*. (a) Cyclic Voltammogram of SC-PB (b) Potassium K-edge XANES of samples held at denoted points during the CV. CV measurements were made using 0.1 M KNO_3 (aq) electrolyte using a scan rate of 0.77 mV/s.

(a)

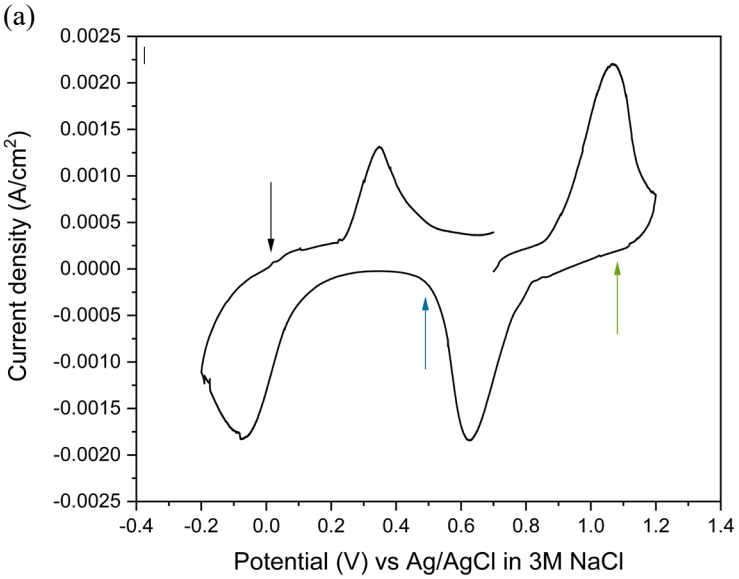

(b)

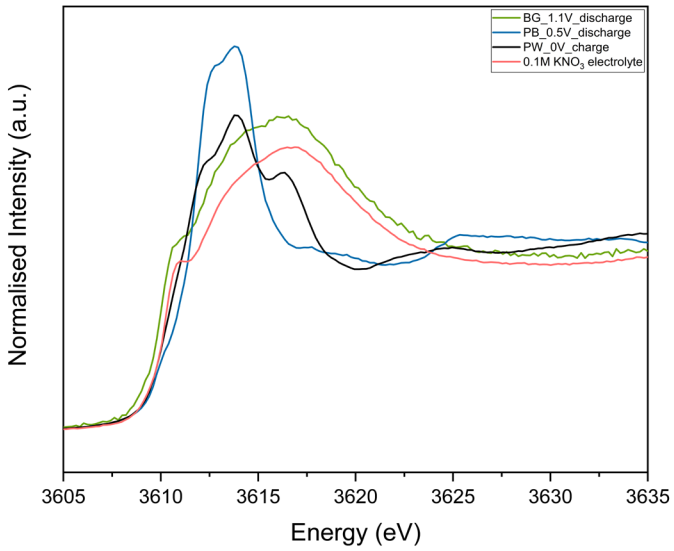

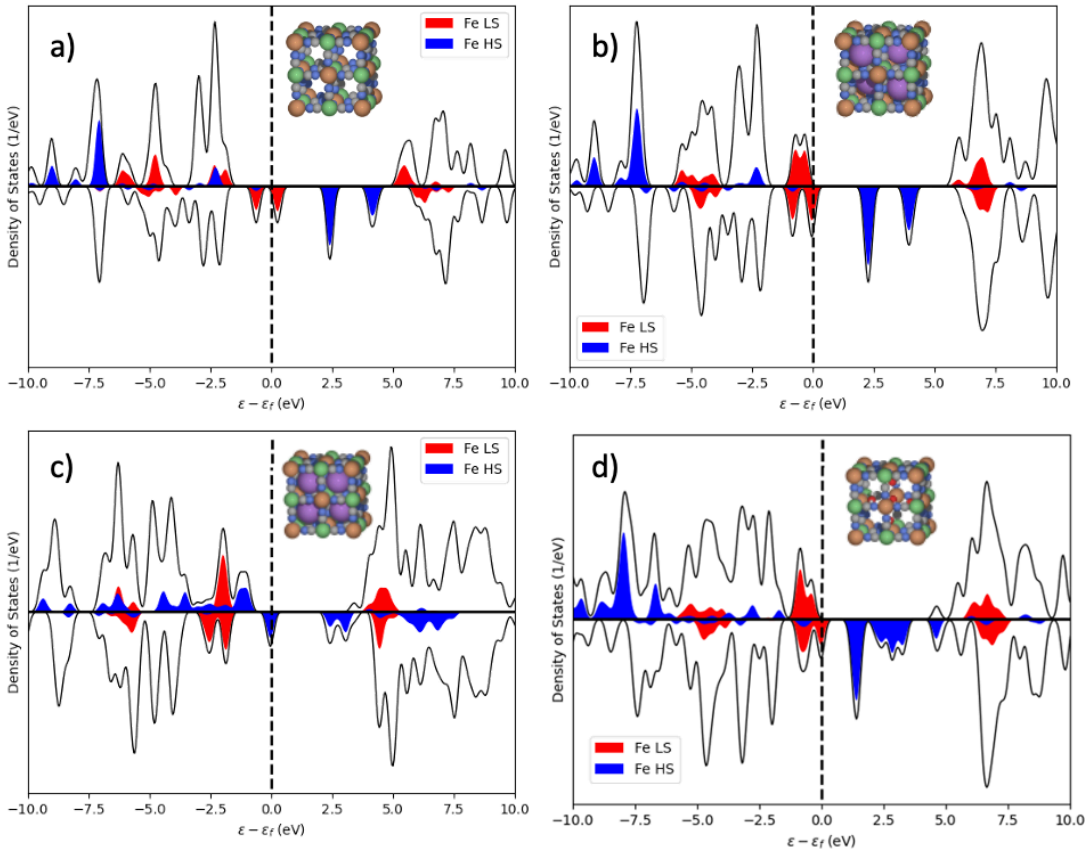

Figure S 13. a) Electronic DOS for a) BG b) PB c) PW d) PW with defect as calculated with DFT (HSE06, Gaussian broadening applied).

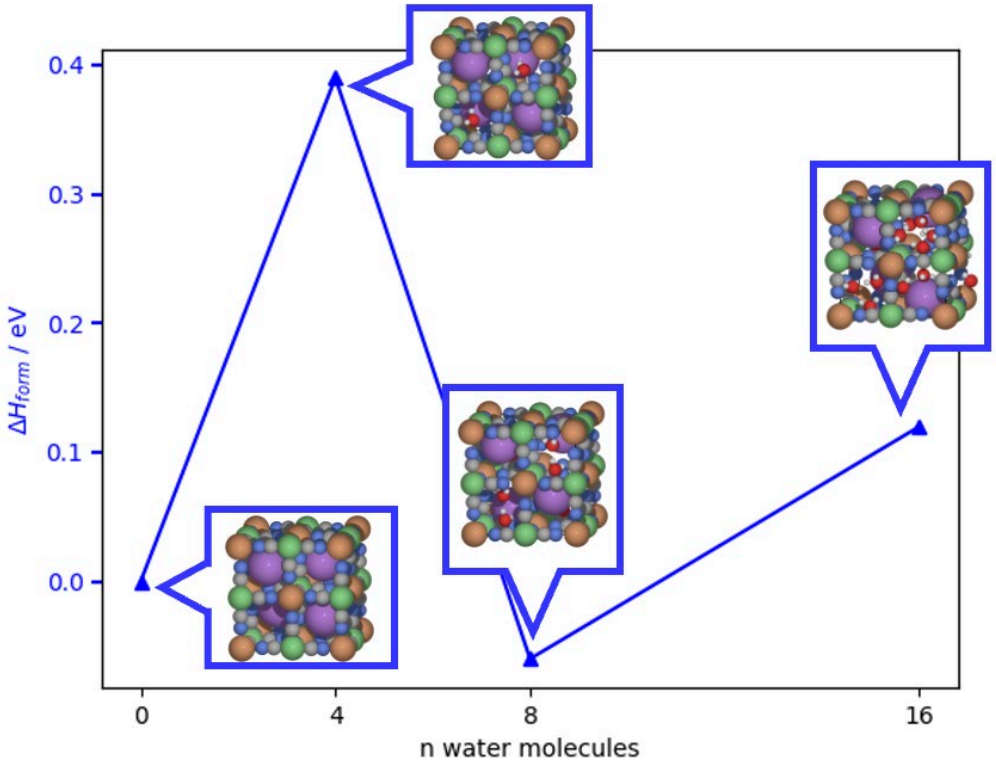

Figure S 14. ΔH_{form} for addition of 4, 8, and 16 H_2O molecules to unit cell of PB as calculated with DFT (HSE06).

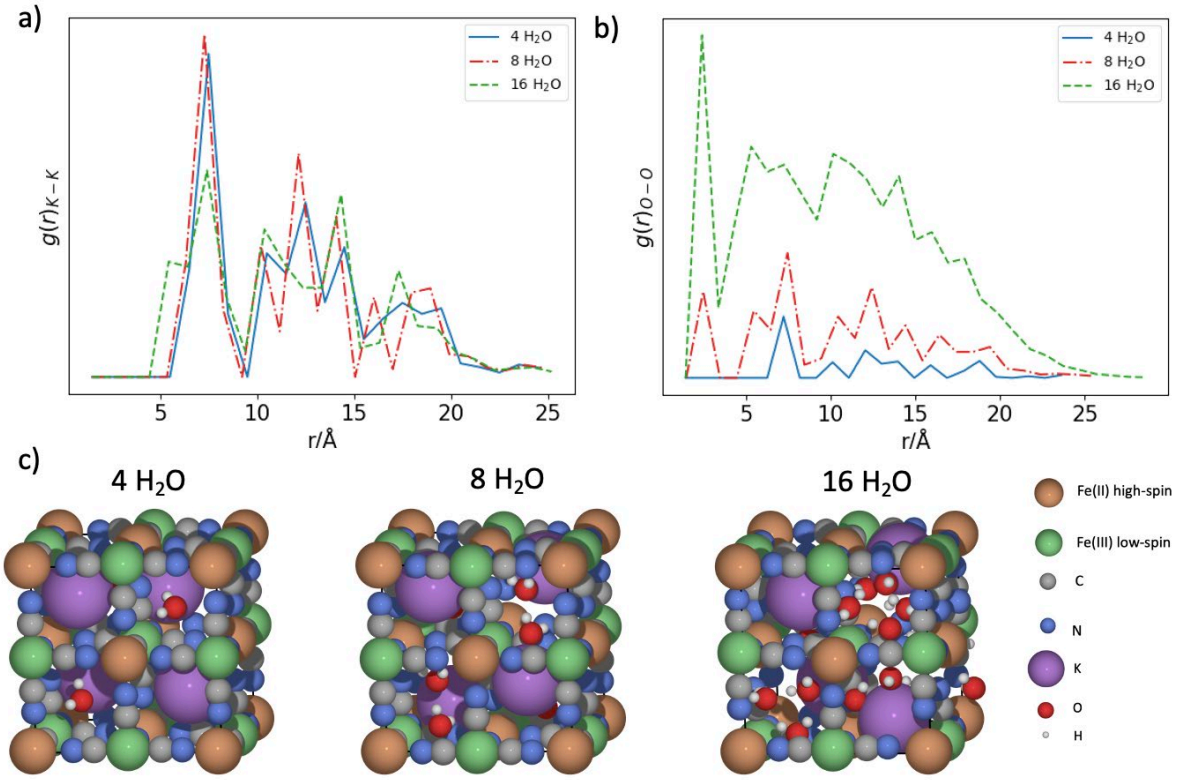

Figure S 15. a) K-K b) O-O RDFS for H_2O of 4 (blue solid line), 8 (red dotted and dashed line), 16 (dashed green line) on structures optimised with PBEsol+TS. c) Structures for PB (Td) for H_2O loadings of 4, 8, 16 molecules.

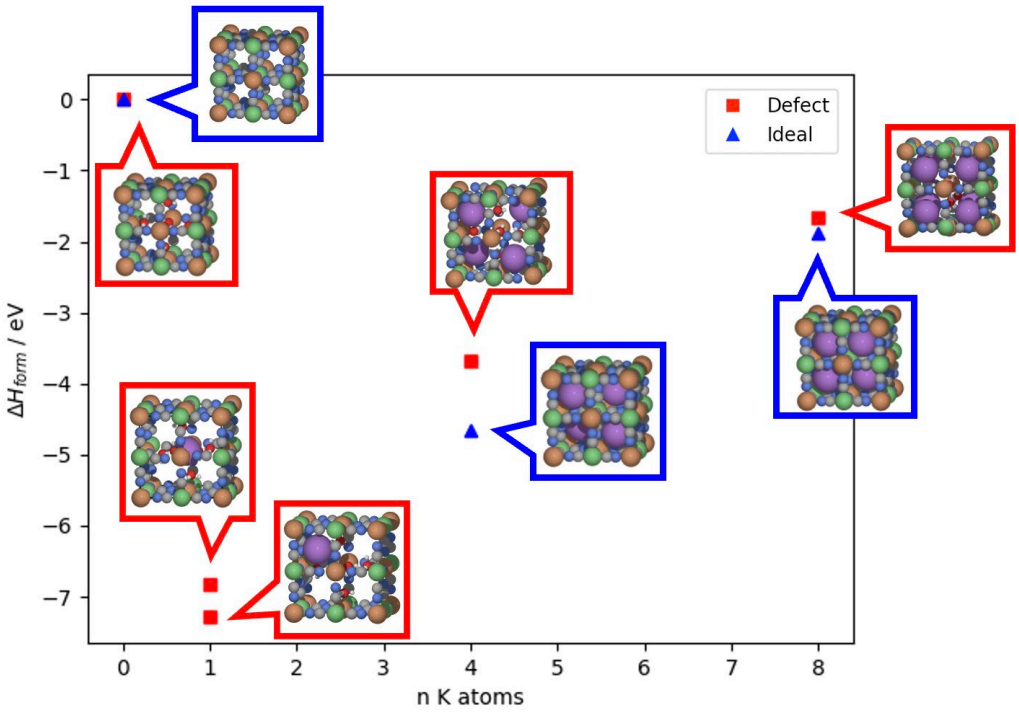

Figure S 16. ΔH_{form} for soluble (blue triangles) and insoluble (reds square) structures as a function of K^+ loadings as calculated with DFT (HSE06).

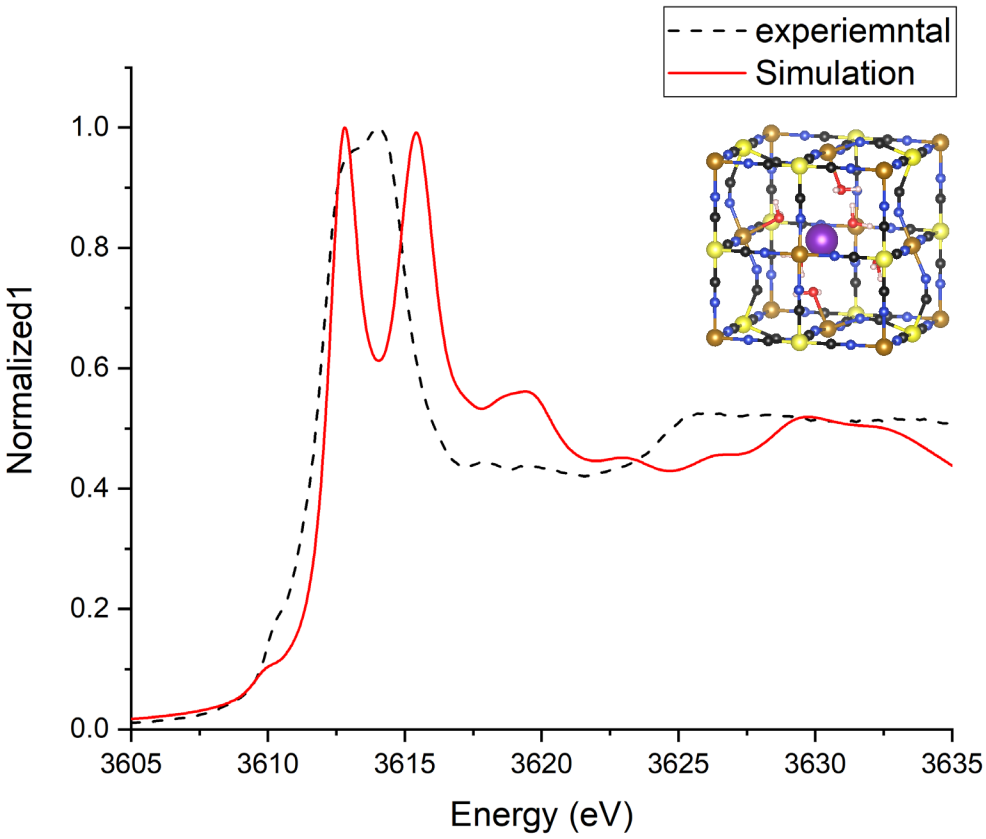

Fig S 17 Simulated potassium K-edge XANES with K^+ siting within the $[(H_2O)_6]$ defect site plane-wave pseudopotential DFT.

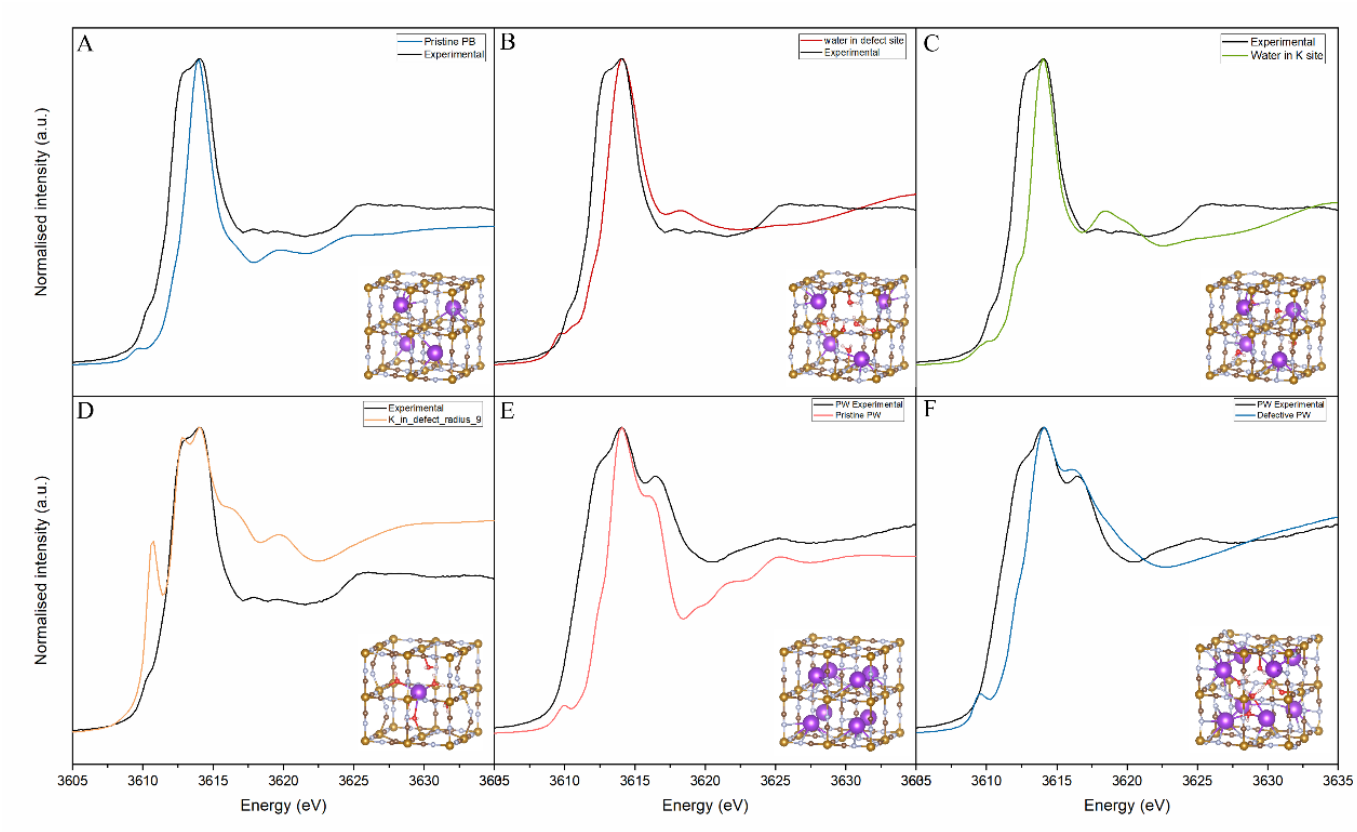

Figure S 18. Finite difference method simulations of potassium K edge XANES using DFT calculated structures of PB vs experimental of C-PB and PW: A) Pristine PB, B) PB with defect site, C) Four interstitial waters in empty 8c sites, D) Potassium in defect site surrounded by water, E) Pristine PW, F) PW with defect site. FDM simulations consistently fail to capture leading edge &/or the relative intensity of edge features when compared to DFT plane-wave calculations.

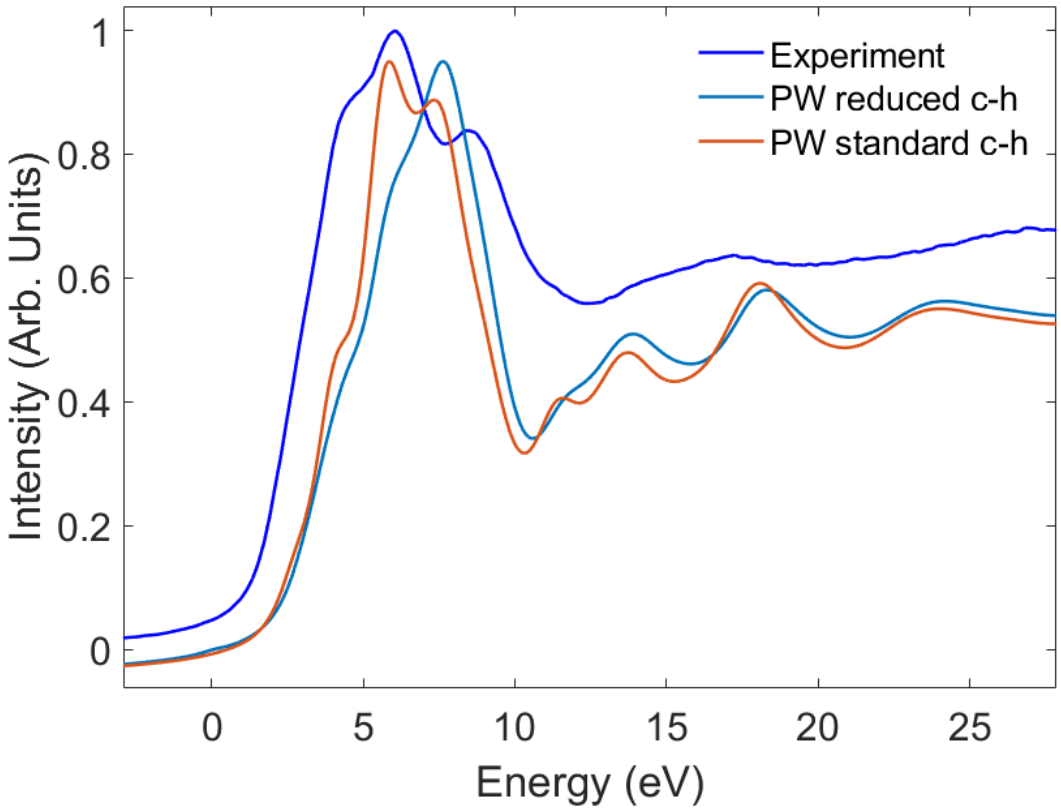

Figure S 19. Simulations of X-ray absorption of Prussian White performed using the plane-wave pseudopotential DFT with adjusted strength of core-hole interaction.

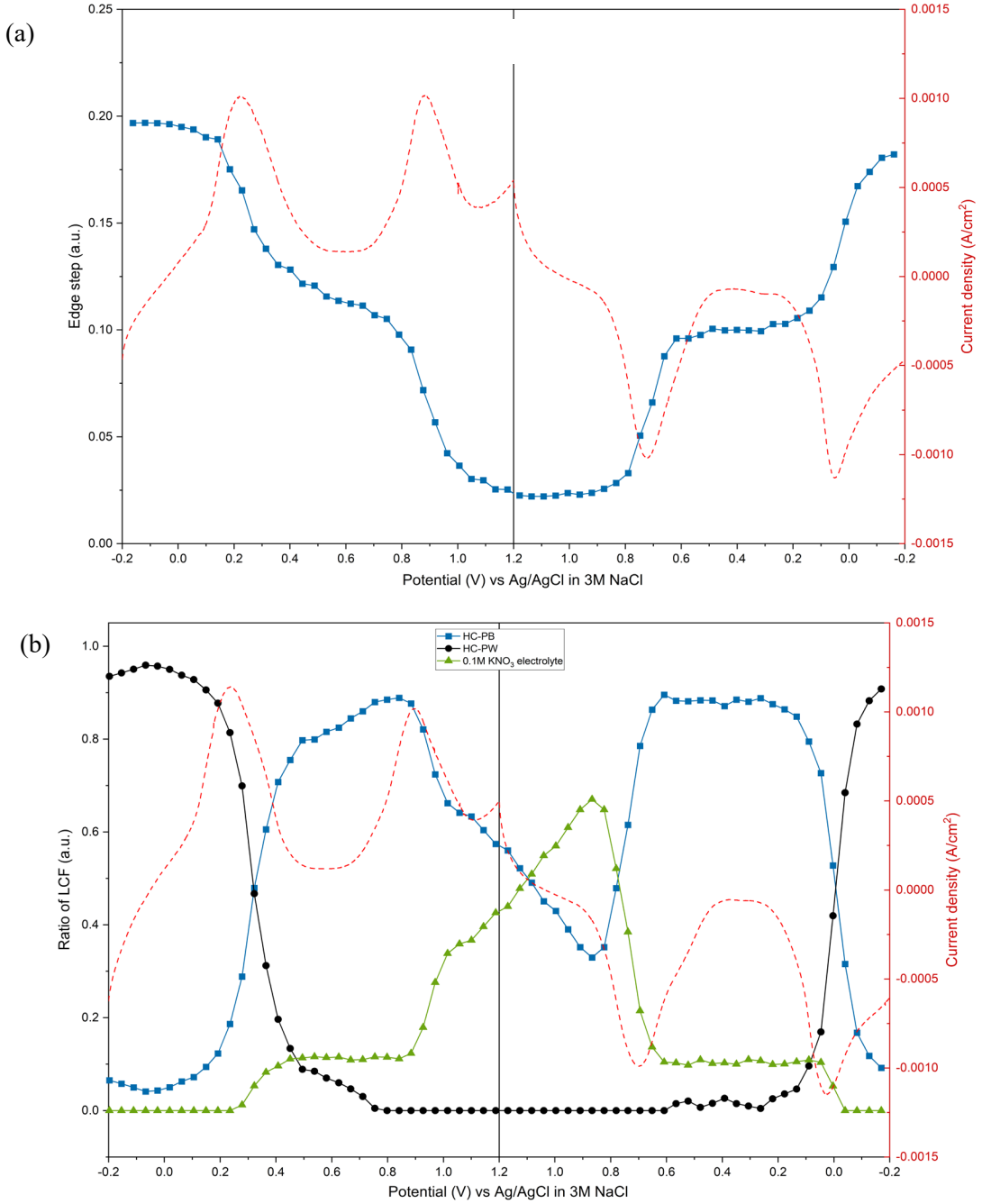

Figure S20. Operando Potassium K-edge XANES of LC-PB during cyclic voltammetry. (a) Comparison of unnormalized XANES edge step value (associated with K^+ concentration) at specific applied potentials and corresponding current density. (b) Comparison of fraction of K^+ species determined from linear combination fitting of normalized XANES.

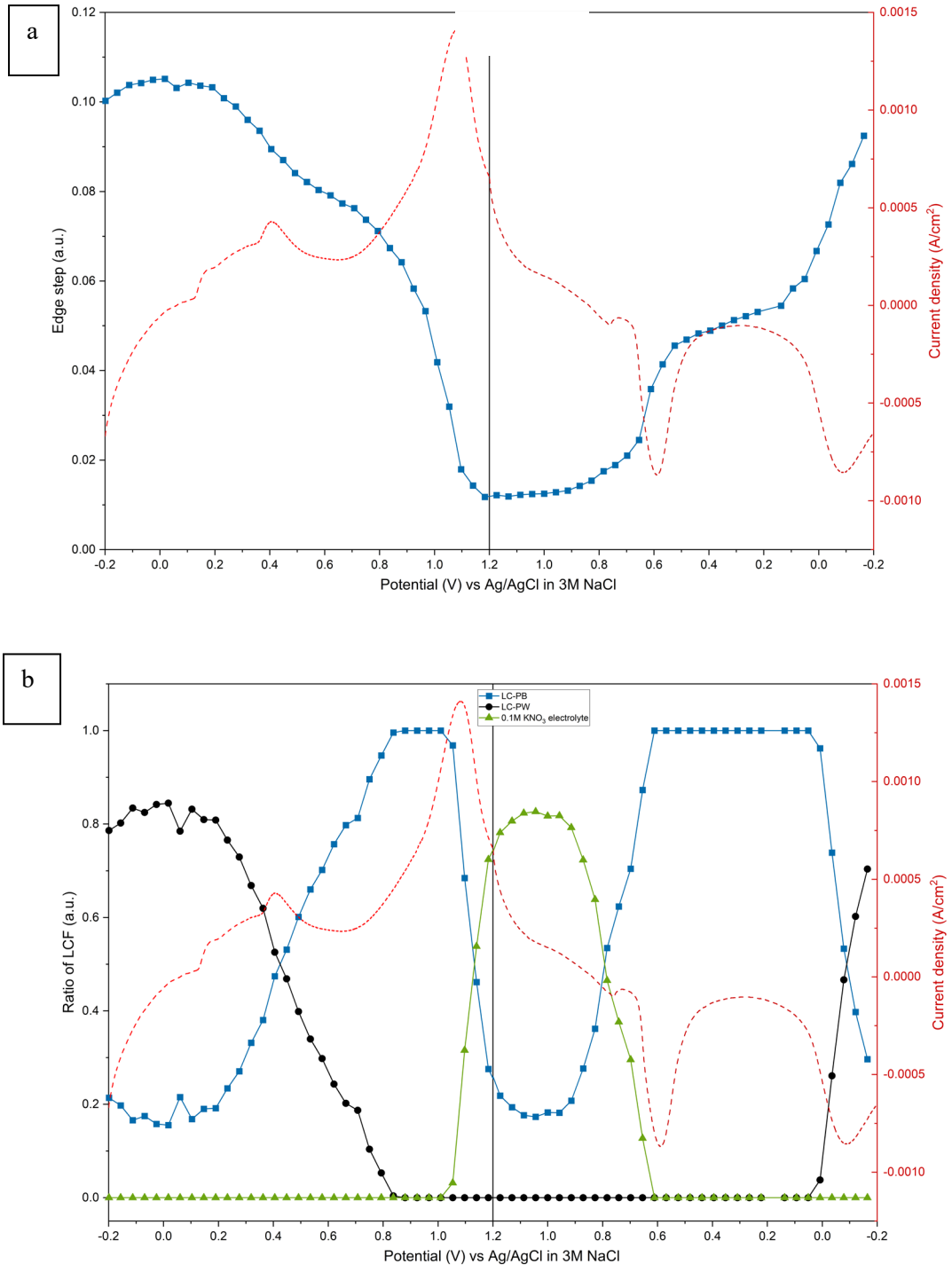

Figure S21. Operando Potassium K-edge XANES of SC-PB during cyclic voltammetry. (a) Comparison of unnormalized XANES edge step value (associated with K^+ concentration) at specific applied potentials and corresponding current density. (b) Comparison of fraction of K^+ species determined from linear combination fitting of normalized XANES.

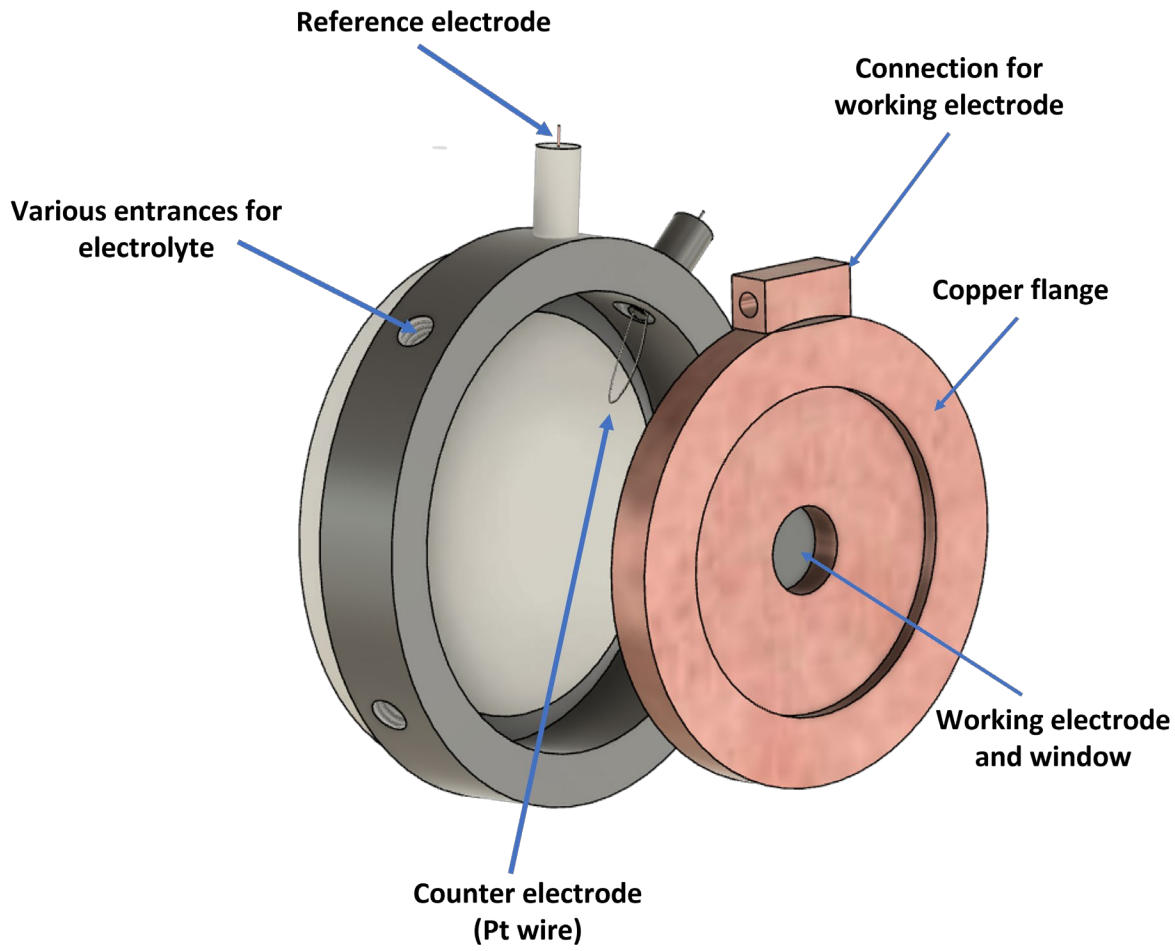

Figure S22. Image of electrochemical cell